A NEW DISCRETE-TIME ANALYTIC SIGNAL FOR REDUCING ALIASING IN DISCRETE TIME–FREQUENCY DISTRIBUTIONS

John M. O' Toole, Mostefa Mesbah and Boualem Boashash

Perinatal Research Centre, University of Queensland,
Royal Brisbane & Women's Hospital, Herston, QLD 4029, Australia.
e-mail: j.otoole@uq.edu.au
web: www.som.uq.edu.au/research/sprcg/

ABSTRACT

The commonly used discrete-time analytic signal for discrete time–frequency distributions (DTFDs) contains spectral energy at negative frequencies which results in aliasing in the DTFD. A new discrete-time analytic signal is proposed that approximately halves this spectral energy at the appropriate discrete negative frequencies. An empirical comparison shows that aliasing is reduced in the DTFD using the proposed analytic signal rather than the conventional analytic signal. The time domain characteristics of the two analytic signals are compared using an impulse signal as an example, where the DTFD of the conventional signal produces more artefacts than the DTFD of the proposed analytic signal. Furthermore, the proposed discrete signal satisfies two important properties, namely the real part of the analytic signal is equal to the original real signal and the real and imaginary parts are orthogonal.

1. INTRODUCTION

TFDs are two dimensional representations of signal energy in the joint time–frequency (t,f) domain [1]. A commonly used class of TFDs is the quadratic shift-invariant TFD class (henceforth referred to as simply TFDs). The most basic TFD of this class is the Wigner-Ville distribution (WVD) defined, for a real signal $s(t)$, as

$$W_z(t,f) = \int_{-\infty}^{\infty} z(t+\tfrac{\tau}{2}) z^*(t-\tfrac{\tau}{2}) \mathrm{e}^{-j2\pi\tau f} \mathrm{d}\tau$$

where $z(t)$ is the analytic associate of $s(t)$ [1, pp. 13]. The reason the analytic associate, $z(t)$, is used rather than real signal $s(t)$ is twofold: firstly it eliminates the crossterms between the positive and negative frequency components in the (t,f) domain and secondly it makes an alias-free discrete-time representation possible [2]. The general form of this class of TFDs can be expressed using the (t,f) kernel $\gamma(t,f)$ as follows:

$$\rho_z(t,f) = W_z(t,f) \underset{t}{*}\underset{f}{*} \gamma(t,f) \tag{1}$$

where $*$ represents the convolution operation.

1.1 Discrete Time–Frequency Distributions

The implementation of TFDs for digital signal processing purposes requires a discrete version of the continuous TFD defined in (1). This requires that both the time t and frequency f arguments in $\rho_z(t,f)$ be discretised. As TFDs are obtained from mapping a time domain signal $s(t)$, then likewise discrete-time, discrete-frequency TFDs need to be obtained from the finite discrete-time signal $s(nT)$ of length N, where T represents the sampling period.

The requirements for an alias-free discrete-time, discrete-frequency TFDs are as follows: a discrete-time TFD requires that a signal with half the Nyquist bandwidth is used, which is the case for the analytic signal [2]. A discrete-frequency TFD requires that a signal with half the time duration is used, that is $s(nT)$ is zero for $N < n \leq 2N-1$ [3]. Thus these two conditions must be combined to produce a discrete-time, discrete-frequency TFD (simply referred to as a discrete TFD, (DTFD)). As the (t,f) kernel γ is independent of the signal, the formation of the discrete WVD (DWVD) will now be examined.

The DWVD for a signal $s(nT)$ can be represented as [4]

$$W_{z_c}(\tfrac{nT}{2}, \tfrac{k}{2NT}) = \sum_{m=0}^{N-1} z_c(mT) z_c^*((n-m)T) \mathrm{e}^{-j2\pi(m-n/2)k/N} \tag{2}$$

for $n = 0,1,\ldots,2N-1$ and $k = 0,1,\ldots,N-1$. This particular DWVD, based on the one proposed in [3], is presented here as it satisfies more desirable mathematical properties than the more common DWVD definition proposed in [5]. The implications, however, arising from the choice of analytic signal are the same regardless of the DWVD definition. The signal $z_c(nT)$, periodic in $2NT$, is defined as

$$z_c(nT) = \begin{cases} z(nT), & 0 \leq n \leq N-1 \\ 0, & N \leq n \leq 2N-1 \end{cases} \tag{3}$$

where $z(nT)$ represents the discrete-time analytic associate of $s(nT)$, which will be discussed in more detail in the next section. The same DWVD can also be expressed in terms of the discrete-frequency domain signal $Z_c(\frac{k}{2NT})$,

$$W_{Z_c}(\tfrac{nT}{2}, \tfrac{k}{2NT}) = \frac{1}{2N} \sum_{l=0}^{2N-1} Z_c(\tfrac{l}{2NT}) Z_c^*(\tfrac{2k-l}{2NT}) \mathrm{e}^{j\pi(l-k)n/N} \tag{4}$$

where $W_{Z_c} = W_{z_c}$ and Z_c is obtained from the discrete Fourier transform (DFT) of z_c.

1.2 Discrete-Time Analytic Signals

The discrete-time analytic signal $z(nT)$ used in (3) is formed using a frequency domain method described in [6]. The method zeros all the discrete frequency domain samples

at negative frequencies. This is achieved by multiplying $S(\frac{k}{NT})$, the DFT of $s(nT)$, by $H(\frac{k}{NT})$. That is, $Z(\frac{k}{NT}) = H(\frac{k}{NT})S(\frac{k}{NT})$, with $H(\frac{k}{NT})$ defined as

$$H(\tfrac{k}{NT}) = \begin{cases} 1, & k = 0 \text{ and } k = \frac{N}{2}, \\ 2, & 1 \le k \le \frac{N}{2} - 1, \\ 0, & \frac{N}{2} + 1 \le k \le N - 1. \end{cases} \quad (5)$$

The analytic signal $z(nT)$ is then obtained by taking the inverse DFT (IDFT) of $Z(\frac{k}{NT})$.

The justification for using this method is now examined, with alternative methods presented. Preceding this, two properties inherent to the continuous-time analytic signal are introduced in the discrete-time context.

The properties were proposed in [6] in order for $z(nT) = z^{(\mathrm{r})}(nT) + jz^{(\mathrm{i})}(nT)$ to be an "analytic-like" discrete-time signal. First, the real part of the discrete-time analytic signal is exactly equal to the original real signal $s(nT)$, i.e.

$$z^{(\mathrm{r})}(nT) = s(nT) \quad \text{for } 0 \le n \le N-1 \quad (6)$$

and second, the orthogonality between the real and imaginary components of the signal is maintained, i.e.

$$\sum_{n=0}^{N-1} z^{(\mathrm{r})}(nT) z^{(\mathrm{i})}(nT) = 0. \quad (7)$$

Alternative methods to creating the discrete-time analytic signal $z(nT)$ of length N include using dual quadrature FIR filters to jointly produce the real and imaginary components of $z(nT)$, as described in [7]. This approach preserves the orthogonality property (7) but will not preserve the original real signal (6) [6]. Another approach is to approximate the Hilbert transform operation $\mathscr{H}[\cdot]$ with an FIR filter [7], as the analytic signal is related to the real signal by the relation $z(nT) = s(nT) + j\mathscr{H}[s(nT)]$. This approach preserves the original real signal (6) but not the orthogonality property (7). Both of these approaches are implemented in the time domain.

A more recent approach has been proposed in [8], which combines the frequency domain method of [6] with the zeroing of a single value of the continuous spectrum in the negative frequency range. This method preserves the original real signal (6) but not the orthogonality property (7).

In comparison, the frequency domain method [6] is particularly attractive for three reasons. Firstly, as the formation of the DWVD requires a latency of N samples, real-time implementation of the analytic signal is not required. Therefore the analytic signal is not constrained to a time domain only realisation. Thus this method has the advantage of exactly zeroing all the samples in the negative frequency range of the discrete spectrum, i.e. $Z(\frac{k}{NT}) = 0$ for $\frac{N}{2} < k \le N-1$, which is not guaranteed using a time domain FIR approach. Secondly, this method uniquely satisfies the two aforementioned properties [6]. Thirdly, this method has a simple implementation [6] in comparison to the other methods, as no filter has to designed or arbitrary frequency point selected [8].

For these reasons, this method has remained a popular approach for forming a discrete-time analytic signal for use in a DWVD (see, e.g. [2]). However, it is worth noting that although $z(nT)$ is completely zero in the negative half of the discrete spectrum (implicit from its definition [6]), $z_c(nT)$ is not. This is because the Fourier transform of the the discrete-time signal $z(nT)$, $Z(f)$, is only zero at the sample points $f = k/NT$ for $N < k \le 2N-1$. As $z_c(nT)$ is of length $2N$, then $Z_c(f)$ will be nonzero for the odd negative frequency sample points $f = (2k+1)/2NT$. Thus the DWVD in (2) is not entirely alias-free. In an effort to reduce this aliasing, a new discrete-time analytic signal will now be introduced.

2. PROPOSED ANALYTIC SIGNAL

The proposed analytic signal is defined as

$$z_p(nT) = \begin{cases} z_a(nT), & 0 \le n \le N-1 \\ 0, & N \le n \le 2N-1 \end{cases} \quad (8)$$

for $n = 0, 1, \ldots, 2N-1$. The signal $z_a(nT)$ is defined as the analytic associate of $z_c(nT)$, obtained using the frequency domain method described in [6]. That is, $Z_a(\frac{k}{2NT}) = H(\frac{k}{2NT})Z_c(\frac{k}{2NT})$, where $H(\frac{k}{2NT})$ is described in (5) with N replaced by $2N$. Taking the IDFT of $Z_a(\frac{k}{2NT})$ results in $z_a(nT)$. The proposed discrete analytic signal is then obtained by forcing $z_a(nT)$ to zero for $N \le n \le 2N-1$.

The two analytic signals can be described completely in the time domain as a function of the real signal $s(nT)$ (of length N) as

$$z_c(nT) = \left[\tilde{s}(nT)u_1(nT) \circledast \hat{h}(nT)\right] u_1(nT) \quad (9)$$

$$z_p(nT) = \left[\tilde{s}(nT)u_1(nT) \circledast h(nT)\right] u_1(nT) \quad (10)$$

where $\tilde{s}(nT)$ is equal to $s(nT)$ periodically extended to length $2N$ and where $\circledast$ represents circular convolution. The function $u_1(nT)$ is defined as a time-reversed and time-shifted step function, described as $u_1(nT) = u((N-1-n)T)$, where $u(nT)$ represents the unit step function. Thus the term $\tilde{s}(nT)u_1(nT)$ is equal to zero padding $s(nT)$ to $2N$. $h(nT)$, of length $2N$, is the IDFT of the transfer function $H(\frac{k}{2NT})$ defined in (5), which equates to

$$h(nT) = \begin{cases} \delta(nT), & n \text{ even}, \\ \frac{j}{N}\cot(\frac{\pi n}{2N}), & n \text{ odd}. \end{cases} \quad (11)$$

where $\delta(nT)$ is the Kronecker delta function, i.e. $\delta(nT) = 1$ if $n = 0$ and 0 for $n \neq 0$. $\hat{h}(nT)$ can be expressed in terms of $h(nT)$ as

$$\hat{h}(nT) = h(nT) + h((n+N)T). \quad (12)$$

Note the neither analytic signals are formed from the output of a time-invariant system, assuming that $\tilde{s}(nT)$ is the input to the system. In other words both systems are time-variant, as shown in (9) and (10).

The two properties discussed in the previous section for discrete-time analytic signals are satisfied by $z_p(nT)$. First, as $z_p(nT) = z_a(nT)$ for $0 \le n \le N-1$ and as $z_a{}^{(\mathrm{r})}(nT) = s(nT)$ (from its definition [6]), then $z_p{}^{(\mathrm{r})}(nT) = s(nT)$. Thus the proposed analytic signal preserves the original signal (6). Second, as $z_a(nT)$ satisfies the orthogonality property [6], and as $z_a{}^{(\mathrm{r})}(nT) = 0$, for $N \le n \le 2N-1$, then the summation of real and imaginary parts is only over $0 \le n \le N-1$ for $z_a(nT)$. From the definition of $z_p(nT)$ (8), as $z_p(nT) = z_a(nT)$ for this range, it can then be concluded that this orthogonality property also holds for $z_p(nT)$.

3. DISCRETE SPECTRAL ANALYSIS

As the two analytic signals, $z_c(nT)$ and $z_p(nT)$, will be compared in terms of energy in the negative frequency half of the discrete spectrum, it may be beneficial to describe them in the discrete-frequency domain. Thus (9) and (10) are formulated in the discrete-frequency domain as follows:

$$Z_c(\tfrac{k}{2NT}) = \left[S(\tfrac{k}{2NT})\hat{H}(\tfrac{k}{2NT})\right] \circledast U_1(\tfrac{k}{2NT}) \quad (13)$$

$$Z_p(\tfrac{k}{2NT}) = \left[S(\tfrac{k}{2NT})H(\tfrac{k}{2NT})\right] \circledast U_1(\tfrac{k}{2NT}). \quad (14)$$

$\hat{H}$ can be expressed in terms of H, with H defined in (5), as

$$\begin{aligned} \hat{H}(\tfrac{2k}{2NT}) &= 2H(\tfrac{2k}{2NT}) \\ \hat{H}(\tfrac{2k+1}{2NT}) &= 0. \end{aligned} \quad (15)$$

$U_1(\frac{k}{2NT})$ is the IDFT of the step function $u_1(nT)$ presented in the previous section. $S(\frac{k}{2NT})$ is the interpolated version of $S(\frac{k}{NT})$ using the DFT method described in [6]

The difference in the definition of the spectral functions Z_c and Z_p (in (13) and (14)) is between $\hat{H}$ and H. The "impulsive" nature of $\hat{H}$ differs from the more constant H, as illustrated in Fig. 1. The convolution with U_1 is due to setting the discrete-time signals $z_c(nT)$ and $z_p(nT)$ to zero between $N \le n \le 2N-1$, as stated in (10) and (8) respectively.

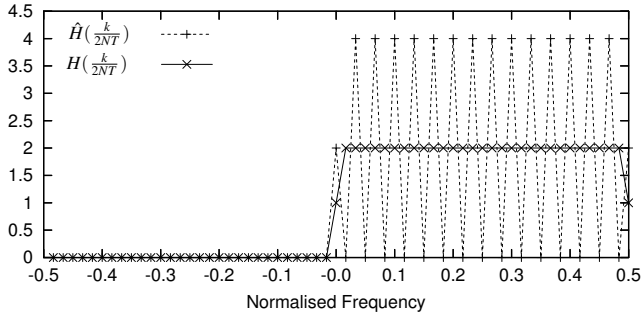

Figure 1: Comparisons of two functions $\hat{H}$, used in the formation of the conventional analytic signal, and H, used in the formation of the proposed analytic signal. This illustrates the simple relationship between the functions described in (15).

The spectral energy at discrete negative frequencies is now examined. Ideally, the analytic signal should be exactly zero in this region. $Z_c(\frac{k}{2NT})$ is zero for even values of k in this region, which is consistent with the definition of $z(nT)$, as $Z_c(\frac{2k}{2NT}) = Z(\frac{k}{NT})$. However, for the odd values of k, $Z_c(\frac{k}{2NT})$ is nonzero. It is proposed that the energy in the negative half of the spectrum for Z_p is approximately half that of Z_c, that is

$$\sum_{k=N+1}^{2N-1} \left|Z_p(\tfrac{k}{2NT})\right|^2 \approx \frac{1}{2}\sum_{k=N+1}^{2N-1} \left|Z_c(\tfrac{k}{2NT})\right|^2. \quad (16)$$

It can be shown (the proof will appear in a future publication and is omitted here for brevity) that for the odd values of k in $Z_p(\frac{k}{2NT})$ the energy, in terms of $Z_c(\frac{k}{2NT})$, is

$$\sum_{k=(N+1)/2}^{(2N-1)/2} \left|Z_p(\tfrac{2k+1}{2NT})\right|^2 = \frac{1}{4}\sum_{k=N+1}^{2N-1} \left|Z_c(\tfrac{k}{2NT})\right|^2. \quad (17)$$

That is, the sum of the spectral energy at negative frequencies for odd values of k only for $Z_p(\frac{k}{2NT})$ is exactly equal to a quarter of the total spectral energy at negative frequencies for all values of $Z_c(\frac{k}{2NT})$ in this region. An expression relating $Z_p(\frac{2k}{2NT})$ in terms of $Z_c(\frac{k}{2NT})$, at negative frequencies, has not been found. However, it will be shown numerically in the next section using a number of signal examples, that the following approximation holds:

$$\sum_{k=(N+1)/2}^{(2N-1)/2} \left|Z_p(\tfrac{2k}{2NT})\right|^2 \approx \sum_{k=(N+1)/2}^{(2N-1)/2} \left|Z_p(\tfrac{2k+1}{2NT})\right|^2.$$

This approximation, coupled with the expression in (17), is required to justify the proposed relationship in (16). It is worth noting that this would not be a valid assumption for Z_c, as it is know that $Z_c(\frac{2k}{2NT}) = 0$, whereas $Z_c(\frac{2k+1}{2NT})$ is usually nonzero, at negative frequencies.

3.1 Empirical Comparison of Analytic Signals

In order to justify the proposed statement in (16) some examples using different signal types will be given. Five different signals types with varied spectral characteristics of different lengths will be used, namely an impulse function, a step function, a sinusoidal signal, a nonlinear frequency modulated signal (NLFM) signal and white Gaussian noise (WGN). The results will be measured in terms of an energy ratio defined as

$$e_r = \frac{\sum_{k=N+1}^{2N-1} \left|Z_p(\tfrac{k}{2NT})\right|^2}{\sum_{k=N+1}^{2N-1} \left|Z_c(\tfrac{k}{2NT})\right|^2}. \quad (18)$$

These results are displayed in the second column in Table 1. For these test signals it is shown that the energy in the negative half of the spectrum of the proposed analytical signal $z_p(nT)$ is approximately half of that for the conventional analytic signal $z_c(nT)$, justifying the proposed statement of (16).

Signal Type	e_r	e_{nr}
Impulse	0.4601	0.6071
Step	0.4675	0.3946
Sinusoid	0.5000	0.5123
NLFM	0.4945	0.4945
WGN	0.4382 (0.042)	0.4425 (0.0413)

Table 1: Ratio of total spectral energy e_r (and normalised spectral energy e_{nr}) in the negative half of the spectrum for the two analytic signals Z_p and Z_c. The length for each signal was arbitrarily set to values between 15 and 2048. For the WGN a 1000 realisations were used and the value is in the form, mean (standard deviation).

To illustrate the differences between the two analytic signals' spectra, the example for the test impulse signal, $s(nT) = \delta(nT)$, is shown in Fig. 2. Note that $|Z_c(\frac{2k}{2NT})| = H(\frac{2k}{2NT})$ (see (5)), as $S(\frac{k}{2NT}) = 1$, for all k. Thus $|Z_c(\frac{2k}{2NT})|^2$ conforms to the ideal spectrum for this particular signal. The problems lies with $|Z_c(\frac{2k+1}{2NT})|^2$, which appears (as illustrated

in Fig. 2) to deviate significantly from the more constant (and ideal) values at $|Z_c(\frac{2k}{2NT})|^2$. Although the proposed magnitude spectrum for Z_p does not attain the ideal either, it produces a more constant, "smoother" magnitude spectrum in comparison to $|Z_c(\frac{k}{2NT})|^2$. It is clear in this example that the spectral energy at negative frequencies for Z_p is less than that for Z_c.

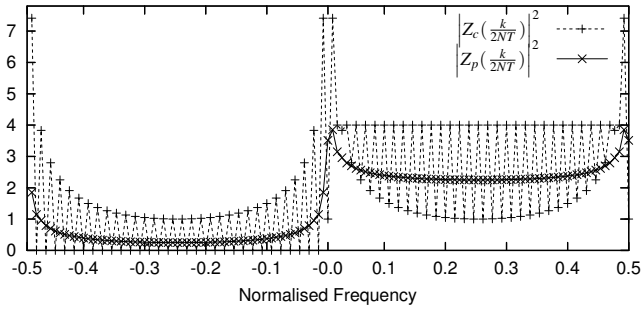

Figure 2: Discrete spectrum of proposed analytic signal $z_p(nT)$ compared with conventional $z_c(nT)$ analytic signal, formed from $s(nT) = \delta(nT)$ of length $N = 64$.

As already stated, the idea of the proposed analytic signal is to reduce the spectral energy at negative frequencies compared with the conventional method. Thus the preceding results justified the approximation in (16). However, as the two analytic signals may have different total energy values, it should also be shown that the normalised spectral energy in this region is likewise reduced, where the normalisation factor is the total signal energy. Thus the new ratio term, in terms of e_r as defined in (18), is

$$e_{nr} = \frac{E_{Z_c}}{E_{Z_p}} e_r \tag{19}$$

where E_{Z_p} represents the total energy for Z_p, e.g. $E_{Z_p} = \sum_{k=0}^{2N-1} |Z_p(\frac{k}{2NT})|^2$ and likewise for E_{Z_c}. The results are displayed in the third column of Table 1 for the same set of signals. Most of the results adhere closely to the values for e_r, as the difference in total energy for the two signals is typically small, with the notable exception being the impulse function. The reason for this is highlighted in Fig. 2, where Z_c appears highly oscillatory in nature compared with Z_p, thus resulting in a larger total energy value.

4. REDUCED ALIASED DWVD

The proposed analytic signal $z_p(nT)$ can be used for the formation of the DWVD. As mentioned previously, one of the requirements for an alias-free DWVD is that the analytic signal is completely zero in the negative frequency range of the spectrum [2]. Thus as both the conventional $z_c(nT)$ and proposed $z_p(nT)$ analytic signals are not exactly zero in this range, some aliasing will occur. To emphasis the advantage of using $z_p(nT)$ over $z_c(nT)$, the extent of this aliasing will be measured and compared.

To assess the aliasing in the DWVD, the two-dimensional spectral "leakage" will be examined in the doppler-frequency (ν, f) domain. The DWVD can be formed from the (ν, f) function, where this function is defined as

$$\mathscr{K}_{Z_c}(\tfrac{l}{2NT}, \tfrac{k}{2NT}) = Z_c(\tfrac{l}{2NT}) Z_c^*(\tfrac{2k-l}{2NT}).$$

This asymmetrical 2D function is summed over $l = 0, 1, \ldots, 2N-1$ in (4) to form the DWVD. Ideally $\mathscr{K}_{Z_c}(\frac{l}{2NT}, \frac{k}{2NT})$ should be zero for $N < l \leq 2N-1$, which would be the case if $Z_c(\frac{k}{2NT})$ was zero for $N < k \leq 2N-1$. In this region, the further away from zero $\mathscr{K}$ deviates the more aliasing will occur in the DWVD, as this nonzero content will be spread about the DWVD after the DFT on $\mathscr{K}$ (as described in (4)). Thus the squared error, summed over this region, should give an indication of the amount of nonzero content present. The following ratio squared error measure, normalised to the total signal's energy, will be used to compare the two analytic signals:

$$e_{\mathscr{K}} = \frac{E_{Z_c} \sum_{k=0}^{N-1} \sum_{l=N+1}^{2N-1} \left| \mathscr{K}_{Z_p}(\frac{l}{2NT}, \frac{k}{2NT}) \right|^2}{E_{Z_p} \sum_{k=0}^{N-1} \sum_{l=N+1}^{2N-1} \left| \mathscr{K}_{Z_c}(\frac{l}{2NT}, \frac{k}{2NT}) \right|^2}.$$

The same five test signals used in Section 3.1 are used to calculate values for $e_{\mathscr{K}}$, the results of which are shown in Table 2. For these test signals is it clear that the amount of nonzero content in the negative doppler half of the (ν, f) function is significantly less for $\mathscr{K}_{Z_p}$ compared with $\mathscr{K}_{Z_c}$. Thus the amount of aliasing present in the DWVD W_{Z_p} will be less than the DWVD W_{Z_c}.

Signal Type	$e_{\mathscr{K}}$
Impulse	0.4774
Step	0.4480
Sinusoid	0.4351
NLFM	0.5077
WGN	0.4822 (0.0859)

Table 2: Ratio of total squared error leaked into the negative doppler half of the (ν, f) function $\mathscr{K}$, using the two different analytic signals. The measure is normalised to the signal's energy. For the WGN a 1000 realisations were used and the value is in the form, mean (standard deviation).

4.1 DTFD Example for Impulse Signal

The proposed analytic signal will be compared with the conventional one in the time domain, using the example of the impulse test signal defined in Section 3.1.

The differences between the time domain signals, as defined in (9) and (10), is described by the relationship in (12). That is, the $\hat{h}(nT)$ function is defined as a folded version of $h(nT)$, which results in undesirable artefacts (or aliasing) in $z_c{}^{(\mathrm{i})}(nT)$. For $s(nT) = \delta(nT)$, the two analytic signals are represented as

$$z_c(nT) = \hat{h}(nT) u_1(nT)$$
$$z_p(nT) = h(nT) u_1(nT)$$

with $z_c{}^{(\mathrm{r})}(nT) = z_p{}^{(\mathrm{r})}(nT) = \delta(nT)$. The imaginary part of $h(nT)$, as defined in (11), tends to zero around $n = N$ and towards $\pm\infty$ at $n = 0$ and $n = 2N-1$ respectively (for the odd n terms only and therefore does reach these singularities). Thus for $z_p{}^{(\mathrm{i})}(nT)$, the main time domain energy is concentrated around $n = 1$ and decreases as n increases.

This is not the case for ${z_c}^{(\mathrm{i})}(nT)$, as the folded function $\hat{h}(nT) = h(nT) + h((N+n)T)$ within $0 \le n \le N-1$, contains energy around $n = 1$ and $n = N-2$. Thus for ${z_c}^{(\mathrm{i})}(nT)$, two significant "components" are present, the effects of which will now be illustrated in the (t, f) domain.

The two DWVDs W_{z_p} and W_{z_c} are displayed in Fig. 3. For W_{z_c}, this second component can be seen as an impulse-type component centred around $n = N-1$. Due to the presence of two components, a cross-term will be present in the DWVD (due to the quadratic nature of the WVD, see, e.g. [1]). This is evident in Fig. 3a where an extra component centred around $n = N/2$ is displayed. In contrast to this, W_{z_p} more closely resembles the ideal DTFD, as shown in Fig. 3b, where the impulse component appears centred around $n = 0$ whilst the remaining area remains empty, or close to zero, as n increases.

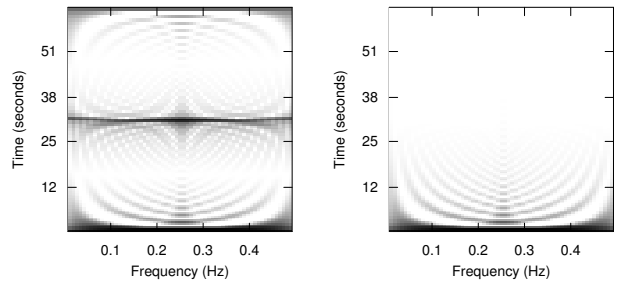

(a) DWVD W_{z_c} (b) DWVD W_{z_p}

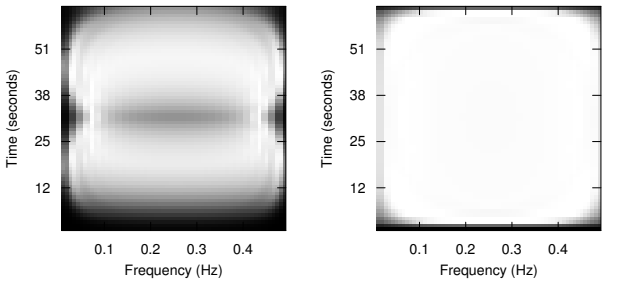

(c) MB distribution ρ_{z_c} (d) CW distribution ρ_{z_c}

Figure 3: DWVD using conventional analytic signal (a) and proposed analytic signal (b). DTFDs for the conventional analytic signal: (c) MB distribution with $\beta = 0.1$ and (d) CW with $\sigma = 10$.

The ability of the DTFD to suppress these unwanted artefacts in W_{z_c} will now be examined. Two different types of DTFDs, namely the modified B (MB) distribution and the Choi-Williams (CW) [1] will be used. Both of these distributions have different (t, f) kernel types $\gamma(\cdot)$ and a different performance is to be expected. As the MB distribution smooths the DWVD by convolving in the time direction only, the oscillatory (in the frequency direction) cross-term is still present, as shown in Fig. 3c. As the CW distribution convolves in both time and frequency, it does a better job at removing the cross-term, as shown in Fig. 3d. However both DTFDs still have a component centred around $n = N-1$. Thus it can be concluded that although the DTFD may suppress these unwanted artefacts, it is dependent on the distribution used and may not always be effective at doing so.

5. CONCLUSION

Any nonzero content at negative frequencies in the discrete spectrum of a discrete analytic signal will introduce aliasing into the DTFD. A new discrete-time analytic signal was proposed, $z_p(nT)$, which was based on a commonly used frequency domain approach [6], $z_c(nT)$. It was shown that $z_p(nT)$ contains approximately half of the total energy at negative frequencies in the discrete spectrum compared with $z_c(nT)$. The amount of aliasing in the DTFD was measured as the amount of spectral leakage in the doppler half of the asymmetrical (ν, f) function. It was empirically shown, in the mean squared error sense, that the amount of spectral leakage for W_{z_p} is approximately half of that for W_{z_c}. The structure of the two analytic signals were also compared in the time domain using the impulse signal as an example. It was observed in the (t, f) domain, for this signal, that ρ_{z_c} contained several artefacts not present in ρ_{z_p} .

Unlike other filter based approaches for generating discrete-time analytic signals, the proposed approach satisfies two important properties and has a simple implementation.

It can also be noted that the discrete-time analytic signal $z_p(nT)$, defined only for $0 \le n \le N-1$, produces an analytic signal for the particular class of signals specified in [8], for which the frequency domain approach of [6] fails. $z_p(nT)$ has the advantage over the approach in [8] in that it satisfies both properties.

REFERENCES

[1] B. Boashash, Ed., *Time-Frequency Signal Analysis and Processing: A Comprehensive Reference*. Oxford, UK: Elsevier, 2003.

[2] B. Boashash, "Note on the use of the Wigner distribution for time-frequency signal analysis," *IEEE Trans. Acoust., Speech, Signal Processing*, vol. 36, no. 9, pp. 1518–1521, 1988.

[3] F. Peyrin and R. Prost, "A unified definition for the discrete-time, discrete-frequency, and discrete-time/frequency Wigner distributions," *IEEE Trans. Acoust., Speech, Signal Processing*, vol. 34, no. 4, pp. 858–866, Aug. 1986.

[4] J. O' Toole, M. Mesbah, and B. Boashash, "A discrete time and frequency Wigner–Ville distribution: properties and implementation," in *Proc. Int. Conf. on Digital Signal Processing and Comm. Systems*, vol. CD-ROM, Dec. 19–21, 2005.

[5] T. Claasen and W. Mecklenbräuker, "The Wigner distribution — a tool for time-frequency signal analysis. Part II: discrete-time signals," *Philips J. Research*, vol. 35, pp. 276–350, 1980.

[6] S. L. Marple, Jr., "Computing the discrete-time 'analytic' signal via FFT," *IEEE Trans. Signal Processing*, vol. 47, no. 9, pp. 2600–2603, 1999.

[7] A. Reilly, G. Frazer, and B. Boashash, "Analytic signal generation—tips and traps," *IEEE Trans. Signal Processing*, vol. 42, no. 11, pp. 3241–3245, 1994.

[8] M. Elfataoui and G. Mirchandani, "A frequency domain method for generation of discrete-time analytic signals," *IEEE Trans. Signal Processing*, vol. 54, no. 9, pp. 3343–3352, 2006.